Nanoscale

PAPER

View Article Online
View Journal

Cite this: DOI: 10.1039/c6nr06504j

Exploiting the interaction between a semiconductor nanosphere and a thin metal film for nanoscale plasmonic devices†

H. Li,‡[a] Y. Xu,‡[b] J. Xiang,[a] X. F. Li,[a] C. Y. Zhang,[c] S. L. Tie[d] and S. Lan*[a]

Received 17th August 2016,
Accepted 17th October 2016

DOI: 10.1039/c6nr06504j

www.rsc.org/nanoscale

The interaction of silicon (Si) nanospheres (NSs) with a thin metal film is investigated numerically and experimentally by characterizing their forward scattering properties. A sharp resonant mode and a zero-scattering dip are found to be introduced in the forward scattering spectrum of a Si NS by putting it on a 50-nm-thick gold film. It is revealed that the sharp resonant mode arises from a new magnetic dipole induced by the electric dipole and its mirror image while the zero-scattering dip originates from the destructive interference between the new magnetic dipole and the original one together with its mirror image. A significant enhancement in both electric and magnetic fields is achieved at the contact point between the Si NS and the metal film. More interestingly, the use of a thin silver film can lead to vivid scattering light with different color indices. It is demonstrated that a small change in the surrounding environment of Si NSs results in the broadening of the resonant mode and the disappearance of the zero-scattering dip. Our findings indicate that dielectric–metal hybrid systems composed of semiconductor NSs and thin metal films act as attractive platforms on which novel nanoscale plasmonic devices can be realized.

1. Introduction

In recent years, silicon (Si) nanospheres (NSs) with diameters ranging from 100 to 250 nm, which exhibit strong electric and magnetic dipole (ED and MD) resonances in the visible to near infrared spectral region, have attracted tremendous interest because they are considered as the most promising building blocks for metamaterials operating at optical frequencies where artificial atoms made of metals fail to work.[1–7] One remarkable feature of such Si NSs is the strong MD induced by a circular current distribution which results in the strong scattering of white light termed "magnetic light".[1] Directional scattering of such Si NSs has been studied in both the microwave and the visible to near infrared spectral regions and it was found that Si NSs exhibit much different forward and backward scattering at specific wavelengths (*e.g.*, the wavelengths satisfying the first and second Kerker's conditions).[4,5,8] The most noteworthy feature is the complete vanishing of backward scattering observed at the wavelength where the first Kerker's condition is fulfilled.[8] In principle, the zero backward scattering originates from the destructive interference between the out-of-phase oscillating ED and MD with equal amplitude.[4,5] In addition, unidirectional light scattering or angular radiation has been achieved by using low-loss dielectric nanoantennas based on Si nanodisk dimers or stair-like single elements.[9,10] Very recently, Fano resonances have been observed in Si NS dimers and core–shell Si NSs,[11,12] which belong to all-dielectric systems, and it was attributed to the interference between the significantly broadened ED and the nearly unbroadened MD of the coupled Si NSs or core–shell Si NSs. In these cases, the Fano resonances were observed near the wavelengths of the MDs. In fact, Fano resonances were also observed in the oligomer of Si or Au NSs owing to the collective interaction between the constituent Si and Au NSs.[13–16]

In general, nanoscale optical components supported by substrates are employed to manipulate, redirect and concentrate light in integrated optics, solar cells and sensors. From the viewpoint of practical application, a systematic study of dielectric resonators on substrates has been carried out and the influence of particle geometry and dielectric environment

[a]*Guangdong Provincial Key Laboratory of Nanophotonic Functional Materials and Devices, School of Information and Optoelectronic Science and Engineering, South China Normal University, Guangzhou 510006, China. E-mail: slan@scnu.edu.cn*
[b]*Department of Electronic Engineering, College of Information Science and Technology, Jinan University, Guangzhou 510632, China*
[c]*School of Physics and Electronic Engineering, Guangzhou University, Guangzhou 510006, China*
[d]*School of Chemistry and Environment, South China Normal University, Guangzhou 510006, China*

†Electronic supplementary information (ESI) available. See DOI: 10.1039/c6nr06504j

‡These authors contributed equally to this work.

on the resonator behavior of single dielectric particle has been revealed.[17] In particular, it was found that strong coupling of a resonator to a dielectric substrate requires a large contact area between the resonator and the substrate. Similarly, the influence of a dielectric substrate on the plasmonic properties of metallic nanoparticles was also investigated both numerically and experimentally in the ultraviolet to the visible spectral range, by using hemispherical gallium nanoparticles as an example.[18] The dependence of the plasmonic spectra on particle size and shape as a function of the illumination angle and the polarization state has been studied.

Apart from single Si NSs and their oligomers, the interaction between a Si NS and a metal film (*i.e.*, a dielectric–metal hybrid system),[19–22] which is in parallel with the study of the interplay between a metal nanoparticle (NP) and a metal film (*i.e.*, a metal–metal system),[23–25] has attracted great interest in recent years. Early in 2006, the influence of a thin metal film on the plasmonic properties of a gold (Au) NP was numerically investigated.[23] After that, the interaction of the localized surface resonance of an Au NP with the propagating surface plasmon polaritons (SPPs) excited on the surface of an Au film was also experimentally studied.[24] Very recently, the gap mode created between an Au NS and an Au film was characterized both numerically and experimentally.[25] Unfortunately, such a gap mode possesses a linewidth of more than 100 nm and only a moderate electric field enhancement. Although plasmonic nanoparticles provide the possibility to confine light on the nanoscale, the collective oscillation of free electrons leads to unwanted Ohmic loss and inevitable heat generation. A clear advantage of utilizing the dielectric nanoparticles for engineering the scattering of light and realizing the confinement of light is their low loss nature in the visible and near-infrared spectrum.[26–28]

Based on the previous studies on the scattering properties of Si and Au NSs, it seems quite interesting to find out whether we can use a thin metal film to engineer the scattering light of Si NSs because Au NSs possess only EDs while Si NSs exhibit both EDs and MDs. In addition, such a dielectric–metal hybrid system is not only interesting for constructing compact plasmonic wavelength demultiplexers but also attractive for realizing thresholdless nanolasers if Si NSs are replaced by GaAs NSs with similar scattering properties but a direct band gap. Previously, the hybrid gap mode between a semiconductor (*e.g.* CdSe) nanowire and a metal (*e.g.* Ag) film, which possess an extremely small effective mode volume, has been employed to realize plasmon lasers.[29]

Actually, some initial studies have been carried out on such a system and the mirror image theory has been proposed to interpret the modification in the scattering spectra observed for Si NSs placed on the metal film.[19–22] In particular, polarization control over electric and magnetic dipole resonances of dielectric nanoparticles on metal films has been realized very recently.[22] It is noticed, however, that only reflection or backward scattering spectra were examined for Si NSs placed on a thick metal film. This is mainly because that characterization of the forward scattering of such a system requires not only a thin metal film (~50 nm) but also an appropriate arrangement of the sample (*i.e.*, placing the sample face downward as shown in Fig. 1). Otherwise, only an objective with a small NA can be used to collect the forward scattering because of the thick glass substrate and the forward scattering is too weak to be detected. For this reason, there is no report on the use of a thin metal film to manipulate the forward scattering of a Si NS which therefore remains to be explored.

In Fig. 1, we show the configuration of the dark-field microscopy used to characterize the forward scattering of a Si NS sticking on a thin metal film (*e.g.* Au film). The ring-shaped white light generated by the diaphragm and focused by the condenser of a dark-field microscope is impinged on the upper surface of the Au film, generating an evanescent wave on the lower surface of the Au film. The Si NS sticking on the lower surface of the Au film will scatter the evanescent wave into the far field, resulting in the forward scattering of the Si NS which will be collected by the objective and directed to a spectrometer for analysis. Such a configuration is quite similar to that of apertureless scanning near field microscopy and the Si NS can be easily excited by laser light focused by the objective.[30] The understanding of the underlying physical mechanism for the modified scattering behavior will be helpful for designing nanoscale sensors and even plasmon lasers.[31–39]

In this article, we report on the creation of a sharp resonant mode and a zero-scattering dip in the forward scattering spectrum of a Si NS by using a thin metal film (Au and Ag films). It was revealed that the sharp resonant mode arises from a new MD induced by the ED and its mirror image while the zero-scattering dip originates from the destructive interference between the new MD and the original MD together with its mirror image. A large enhancement in both the electric and magnetic fields is achieved at the contact point between the Si NS and the metal film. More interestingly, we showed that the

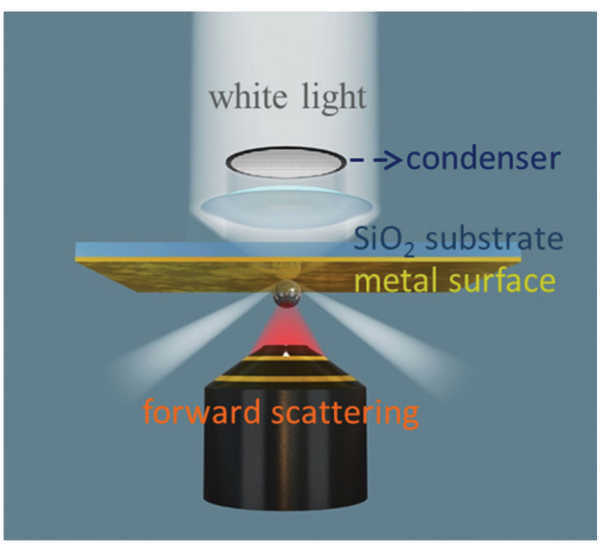

Fig. 1 Schematic showing the dark-field microscopy used to characterize the forward scattering of a Si NS placed on an Au/SiO_2 substrate.

use of a thin Ag film can lead to vivid scattering light with different color indices. The linewidth of the resonant mode and the existence of the zero-scattering dip were found to be quite sensitive to the surrounding environment of the Si NSs. The broadening of the resonant mode as well as the disappearance of the zero-scattering dip was observed when the Si NSs were coated with platinum (Pt) or immersed in water. Our findings indicate potential applications of such a system in nanoscale plasmonic devices such as displayers, demultiplexers, sensors, and even lasers.

2. Experimental and numerical methods

Silicon NSs with different diameters ranging from 100 to 250 nm were fabricated by using femtosecond (fs) laser ablation.[40] A fs laser amplifier (Legend, Coherent) with a pulse duration of 100 fs and a repetition rate of 1 kHz was employed to ablate the Si wafer which was immersed in alcohol. The as-prepared Si NSs were dispersed on Au/SiO_2 and SiO_2–SnO_2/Ag/SiO_2 substrates and their forward scattering spectra were measured by using a conventional dark-field microscope (Observer A1, Zeiss) equipped with a spectrometer (SR-500i-B1, Andor) and a charge-coupled device (DU970N-BV, Andor) for spectra analysis, as schematically shown in Fig. 1. In experiments, we first measured the scattering spectrum of the background at the places without any Si NSs. Then, the scattering spectra of the Si NSs of different diameters were measured. Finally, the scattering spectra of Si NSs were obtained by subtracting the spectrum of the background. The morphologies of the Si NSs were examined by using scanning electron microscopy (SEM) after the measurements of the scattering spectra.

In order to gain a deep insight into the experimental observations, we used the FDTD technique to calculate the scattering spectra and the electric (magnetic) field distributions of Si NSs.[41] A non-uniform mesh with the smallest size of 0.5 nm as well as a perfectly matched boundary was employed in the numerical simulations.

3. Results and discussion

3.1. Forward scattering of Si NSs modified by a thin metal film: numerical simulation

The scattering properties of a Si NS, including scattering intensity and spectral shape, can be greatly modified by using a thin metal film. For a 50-nm-thick Au film placed just behind the Si NS, the intensity of the backward scattering is ~42 times stronger than that of the forward scattering. In contrast, the intensity of the forward scattering is much stronger (~27 times) than that of the backward scattering if the Au film is placed just before the Si NS (see Fig. S1†). In both cases, the scattering spectra appear to be different in the forward and backward directions. Physically, the effects of the thin metal film shown in Fig. 1 are threefold. First, an evanescent wave (near field), which will be scattered by the Si NS into far field, is generated on the lower surface of the metal film upon the illumination of white light. Secondly, a strongly localized mode will be created at the contact point between the Si NS and the metal film. Thirdly and most importantly, the metal film will introduce mirror images for both the ED and the MD of the Si NS based on the mirror image theory and the scattering spectrum is ultimately determined by the coherent interaction between the ED and MD of the Si NS and their mirror images.[19,21] It will be shown later that the cooperation of these effects leads to the formation of the sharp resonant mode and the zero-scattering dip observed in the forward scattering spectrum of the Si NS.

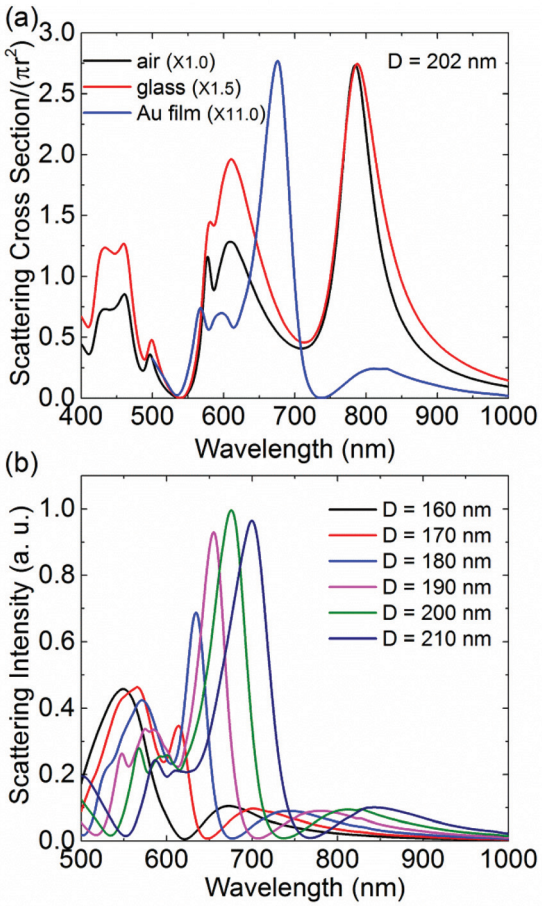

Fig. 2 (a) Forward scattering spectra calculated for a Si NS placed on a glass and an Au/SiO_2 substrate, respectively. The scattering spectrum of the Si NS in the absence of substrate is also provided for comparison. The illumination direction is along the surface normal. For the Si NSs on the glass and Au/SiO_2 substrates, the maximum scattering cross sections are made to be the same as that of the Si NS in air by multiplying different factors. (b) Forward scattering spectra calculated Si NSs with different diameters placed on the Au/SiO_2 substrate. The incidence angle of the illumination light form air to the Au/SiO_2 substrate was chosen to be 53°. The maximum scattering intensities of Si NSs with different diameters are normalized to that of the Si NS with D = 200 nm which exhibits the strongest scattering intensity.

We first calculated the scattering spectrum of a Si NS with a diameter of D = 202 nm placed on an Au/SiO_2 substrate with a 50-nm-thick Au film by using the finite-difference time-domain (FDTD) method, as shown in Fig. 2(a). In this case, white light is incident normally on the Au film. The scattering spectra of the same Si NS in an air background and placed on a glass slide are also provided for comparison. As compared with the Si NS in the air background, the change in the scattering spectrum is very small when the Si NS is put on the glass slide. However, a dramatic change in the scattering spectrum is found when the Si NS is put on the Au film. The most remarkable feature is the sharp resonant mode appearing at ~680 nm. It possesses a narrow linewidth and an asymmetric lineshape. On the long-wavelength side of the resonant mode, a zero-scattering dip is observed at ~740 nm. These two features make the scattering spectrum completely different from those observed in the air background or on the glass slide. As will be shown later, the sharp resonant mode and the zero-scattering dip originate from the coherent interaction between the ED and MD of the Si NS and their mirror images. Therefore, the Au film must be thick enough so that the mirror image theory is applicable. Otherwise, the sharp resonant mode and the zero-scattering dip will not be observed (see Fig. S2†). On the other hand, the scattering light intensity drops rapidly with the increase of the film thickness which makes the measurement of the scattering film thickness which makes the measurement of the scattering light quite difficult. As a tradeoff, an appropriate thickness of ~50 nm was determined for the metal film.

We calculated the forward scattering spectra for Si NSs with different diameters, as shown in Fig. 2(b). In these cases, the light is incident on the SiO_2 substrate at an angle of ~53° which is close to the incidence angle adopted in the measurements of the scattering spectra by using dark-field microscopy. Thus, the incidence angle on the Au film is estimated to be ~33° and no SPPs propagating on the surface of the Au film will be excited. The forward scattering of the Si NS is detected by using a power monitor placed in front of the Si NS. It is confirmed that the resonant mode and the zero-scattering dip remain nearly unchanged for incidence angles smaller than 30° (see Fig. S3†). Therefore, the scattering spectra obtained by normal incidence will be used in the following. For Si NSs with D > 160 nm, the resonant mode as well as the zero-scattering dip begins to appear in the scattering spectrum. With the increasing diameter of Si NSs, a redshift of the resonant mode as well as the zero-scattering dip is observed. The peak intensity of the resonant mode increases firstly with the increasing diameter of Si NSs. However, it begins to decrease when the

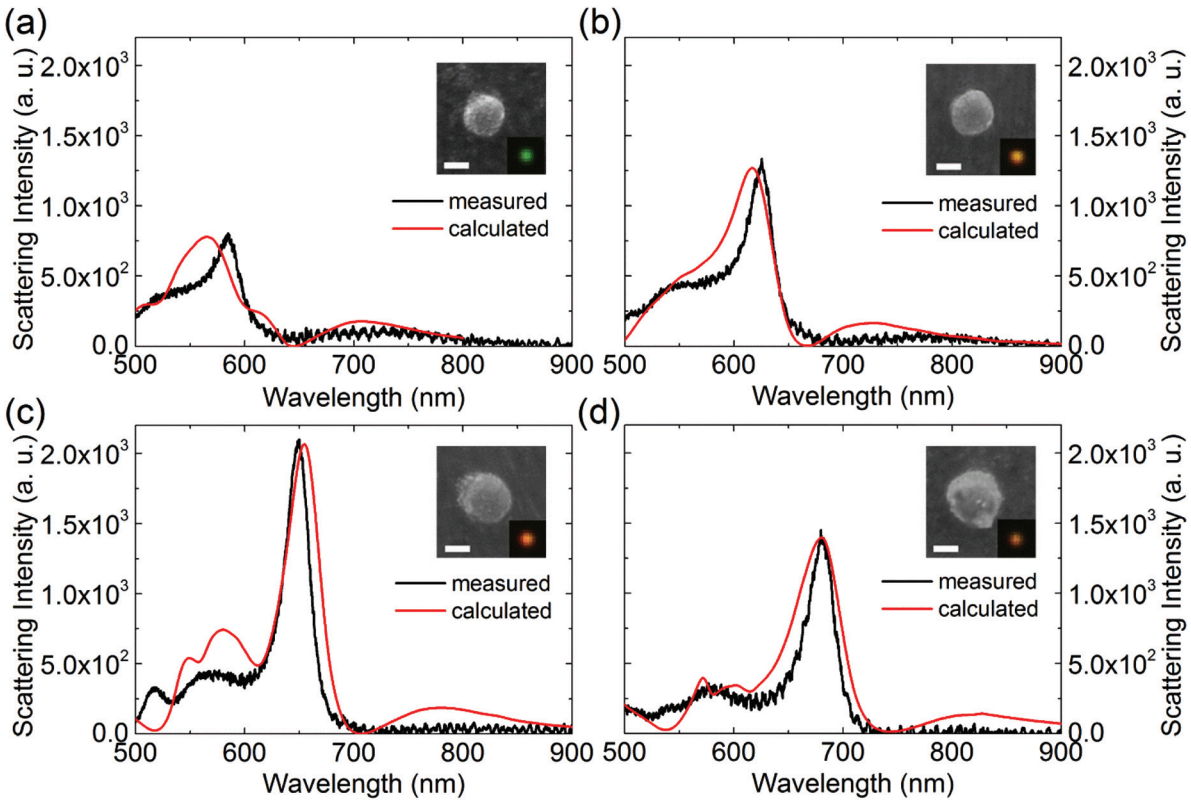

Fig. 3 Forward scattering spectra measured for Si NSs with different diameters placed on the Au/SiO_2 substrate. (a) D = 172 nm, (b) D = 175 nm, (c) D = 185 nm, and (d) D = 202 nm. In each case, the images of the corresponding Si NS obtained by using SEM and dark-field microscopy are provided as insets. The calculated results which resemble the measurement conditions are also provided. In each case, the maximum scattering intensity of the calculated spectrum is made to be the same as that of the measured spectrum in order to make a comparison between the two spectra.

diameter of Si NSs exceeds 210 nm because of the smaller transmissivity of the Au film at long wavelengths. The narrowest linewidth of the resonant mode, which is derived to be ~28 nm, is observed for the Si NS with D = 180 nm.

3.2. Forward scattering of Si NSs modified by a thin metal film: experimental observation

In order to confirm the simulation results, the forward scattering spectra of several Si NSs sticking on an Au/SiO_2 substrate were examined, as shown in Fig. 3 [see also Fig. S4(a)†]. The scanning electron microscopy (SEM) images of the corresponding Si NSs, from which their diameters were estimated, are presented in the insets. In each case, we also show the picture of the scattering light whose color depends strongly on the diameter of the Si NS. The calculated spectra for the Si NSs based on the FDTD simulation are also provided for comparison and a very good agreement between the experimental observations and the simulation results is observed. For the Si NS with D ~ 185 nm, a linewidth as narrow as ~25 nm is observed for the resonant mode [see Fig. 3(c)] which also exhibits the strongest scattering intensity. In order to further validate the engineering of scattering light by using a thin metal film, we examined the modification of the forward scattering spectra of Si NSs by using a 50-nm-thick Ag film with an anti-oxidation coating [see Fig. S4(b)†]. In this case, a 20-nm-thick dielectric layer (SiO_2–SnO_2) with a refractive index of ~1.7 was coated on the Ag film. In Fig. 4(a), we show typical scattering spectra measured for several Si NSs with different diameters. The pictures of the scattering light are presented as insets where vivid colors are observed because of the sharp resonant modes which completely dominate the scattering spectra. The color indices calculated based on the scattering spectra are also presented in the inset, indicating clearly that Si NSs can exhibit distinct colors with the "help" of a thin Ag film. Similar to the photon trapping and emission devices realized by using defects created in two-dimensional photonic crystals,[42] the distinct colors exhibited by Si NSs with different diameters on the thin Ag film are quite attractive for building compact wavelength demultiplexers for SPPs. In Fig. 4(b), we present a comparison of the scattering spectra of two Si NSs with similar diameters placed on the Au and Ag films. As compared with the scattering spectrum of the Si NS placed on the Au film, the resonant mode for the Si NS placed on the Ag film is slightly broadened. However, the relative intensities of the ED and magnetic quadrupole (MQ) resonances with respect to the resonant mode are further reduced. As a result, the scattering spectrum becomes dominated by the resonant mode which exhibits a distinct color. In principle, the modification in the scattering properties is mainly determined by the complex refractive index of the thin film (see Fig. S5†). It is the difference in the complex refractive index that leads to the different modification in the scattering properties which is clearly reflected in the scattering light.

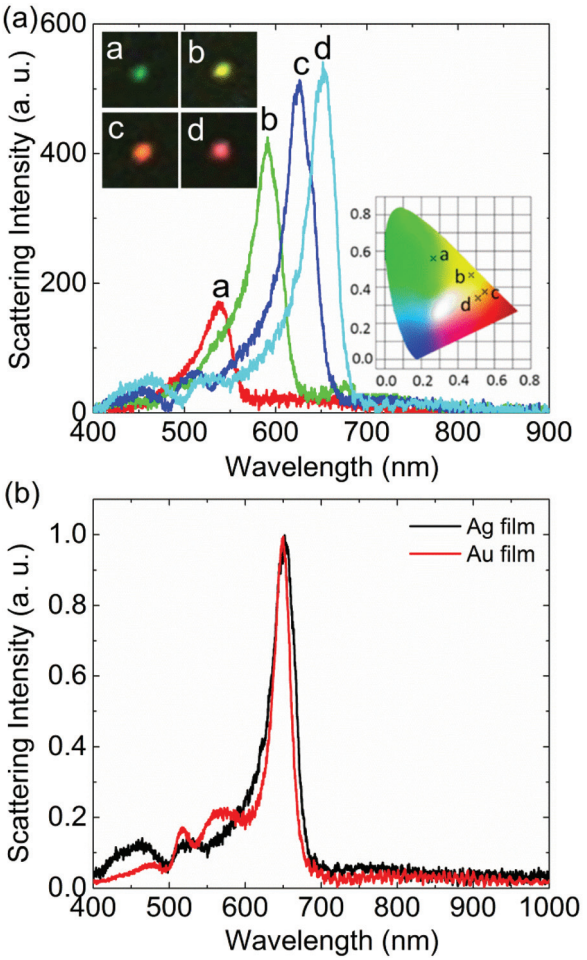

Fig. 4 (a) Scattering spectra of four Si NSs with different diameters placed on the SiO_2–SnO_2/Ag/SiO_2 substrate. The pictures of scattering light and the color indices calculated based on the scattering spectra are provided as insets. (b) Comparison of the scattering spectra of two Si NSs with similar diameters placed on the Au/SiO_2 and SiO_2–SnO_2/Ag/SiO_2 substrates, respectively.

3.3. Physical origin for the sharp resonant mode and zero-scattering dip

In Fig. 5(a), we present a comparison between the calculated and the measured scattering spectra for a Si NS with D = 202 nm. Based on the calculated electric field distributions, we have identified the electric quadrupole (EQ), ED and MD nature for the scattering peaks appearing at 575, 600, and 825 nm, respectively. Now we need to clarify the physical origins for the resonant mode at ~680 nm and the zero-scattering dip at ~740 nm. As mentioned above, the SPPs propagating on the meal surface is not excited under the experimental conditions for measuring the scattering spectra. In principle, the scattering of a Si NS placed on a metal film can be considered as the coherent interaction between the electromagnetic resonances of the Si NS and their mirror images. In the case of normal incidence, the major ED induced by the incident light is the one excited in the Si NS. Apparently, the ED and its

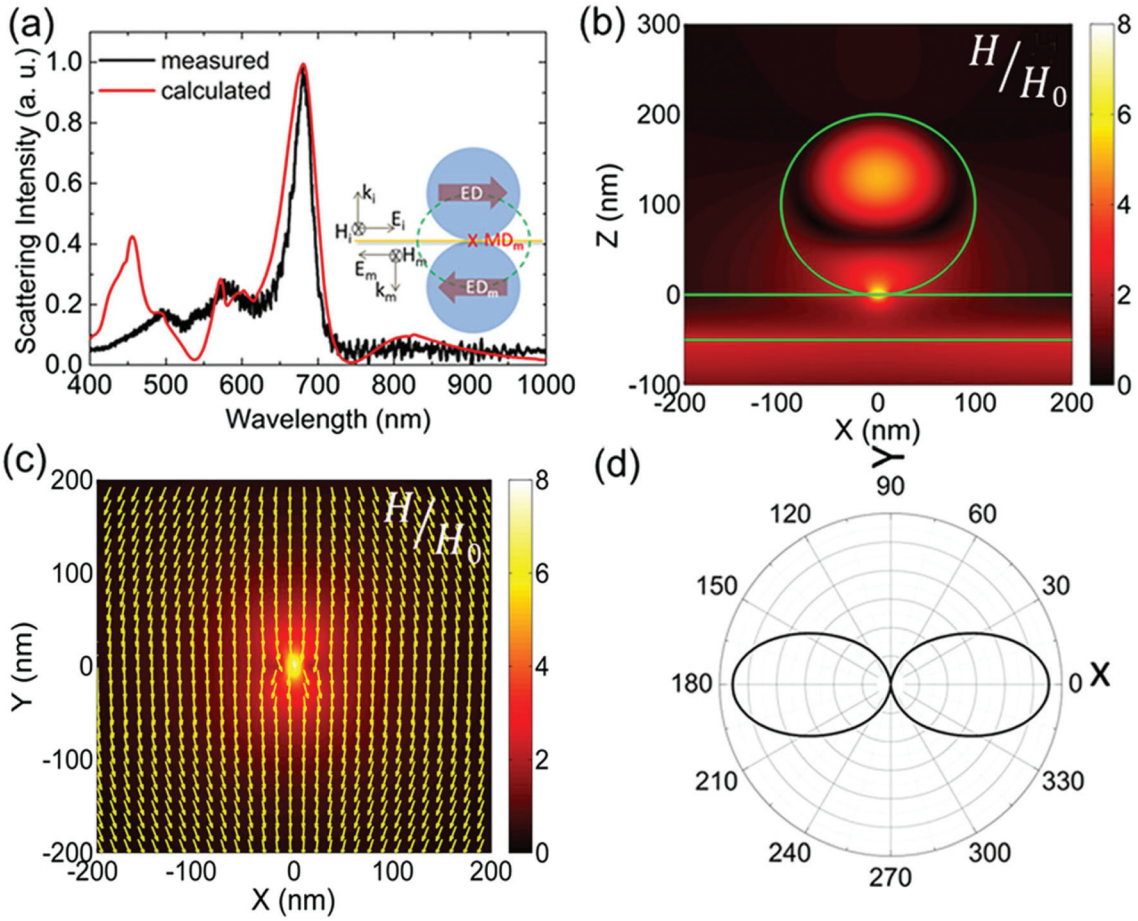

Fig. 5 (a) Comparison of the measured and calculated scattering spectra for a Si NS with a diameter of 202 nm placed on the Au/SiO_2 substrate. The schematic showing the excited ED and its mirror image and the MD_m is presented in the inset. (b) and (c) Magnetic field distributions on the XZ and XY planes calculated at the peak of the resonant mode (680 nm). The scale bar shows the magnetic field enhancement. (d) Scattering pattern on the XY plane calculated at the peak of the resonant mode (680 nm).

mirror-image are antiparallel and separated by a distance equal to the diameter of the Si NS [see Fig. 5(a)]. According to the mirror image theory, these two antiparallel EDs will result in a MD in the middle of them with its orientation perpendicular to them.[19,21] In the far field, the radiation of the two EDs is equivalent to that of the mirror-image-induced MD (MD_m). Therefore, it becomes clear that the resonant mode observed in the modified scattering spectrum originates from the radiation of the new MD induced by two antiparallel EDs, *i.e.*, the MD_m. It is quite similar to that observed in the reflection spectrum of a Si NS placed on a thick metal film.[19] For a Si NS, the scattering is mainly determined by the coherent interaction between the ED and MD. If the ED and MD are in phase, the destructive interference occurs in the forward direction when their amplitudes are equal (*i.e.*, the second Kerker's condition).[8] Similarly, the destructive interference happens in the backward direction when the ED and MD are out of phase and have the same amplitude (*i.e.*, the first Kerker's condition).[8] In our case, the forward scattering is determined by the coherent interaction between the MD_m and the original MD together with its mirror image, as shown in the inset of Fig. 5(a). They are in phase but are located at different positions. Since the MD of a Si NS appears at a wavelength equal to nD,[1] the distance between the MD_m and the original MD (*i.e.* nD/2), which is equal to the radius of the Si NS, corresponds to a phase shift of ~π. The separation between the original MD and its mirror image is equal to the diameter of the Si NS, corresponding to a phase shift of ~2π. For this reason, we can conclude that the radiation of the MD_m and that of the original MD (or its mirror image) are out of phase at a certain frequency in far field. The destructive interference between them is responsible for the zero-scattering dip observed in the forward direction.

In order to verify the formation of the MD_m, we have calculated the magnetic field distributions on the XZ and XY planes at the peak of the resonant mode (680 nm), as shown in Fig. 5(b) and (c). A strong localization of the magnetic field is observed at the contact point between the Si NS and the Au film [see Fig. 5(b)], implying the existence of a MD whose dipole moment is perpendicular to the XZ plane. It is further

confirmed by the magnetic field distribution on the XY plane shown in Fig. 5(c). The formation of the MD_m is also supported by the scattering pattern calculated on the XY plane, as shown in Fig. 5(d). It indicates clearly the existence of a MD at the contact point which oscillates along the Y direction. The electric and magnetic field distributions calculated at the zero-scattering dip were also examined (see Fig. S6†).

In Fig. 3(c) and 5(a), it is noticed that the measured linewidth of the resonant mode is even narrower than the calculated one. It is thought that the shape of Si NSs may affect the linewidth of the resonant mode. In order to confirm this, we have calculated the scattering spectra of Si nanoellipsoids (NEs) with different long and short axes (see Fig. S7†). It can be seen that for Si NEs with a long axis parallel to the Au film, the linewidth of the resonant mode becomes narrower with the increasing long axis. For a Si NE with its long axis parallel to the Au film, a stronger ED will be induced by the incident light as compared with a Si NS or a Si NE with its short axis parallel to the Au film. This behavior is quite similar to the excitation of the longitudinal and transverse surface plasmon resonances of an Au nanorod. The ED parallel to the long axis of the Au nanorod is much stronger than that parallel to the short axis. With this picture in mind, it is understood why a strong resonant mode with a narrow linewidth can be achieved in a Si NE with its long axis parallel to the Au film.

3.4. Application of the dielectric–metal hybrid system in nanoscale sensors

For practical applications, dielectric nanoantennas formed by high refractive index nanoparticles were first proposed for surface-enhanced spectroscopy and their near- and far-field optical properties have been investigated theoretically.[26,27] The electric and magnetic field enhancements provided by Si or GaP dimers have been evaluated and compared with those provided by Au dimers. As compared with their metallic counterparts, a clear advantage of such dielectric nanoantennas is the small heat generation and Si nanoantennas producing surface-enhanced fluorescence and Raman scattering with a negligible temperature increase in the hot spots and surrounding environments have been experimentally demonstrated.[28]

Previously, it has been shown that the Si nanoparticles can be employed as a Raman scattering enhancer for the attached organic molecules because of the strong evanescent electromagnetic fields achieved at the electric and magnetic resonances.[43] Very recently, it has been demonstrated that intensity-shift sensors based on Si NS dimers possess much higher sensitivity than the plasmonic wavelength-shift sensors.[44] In our

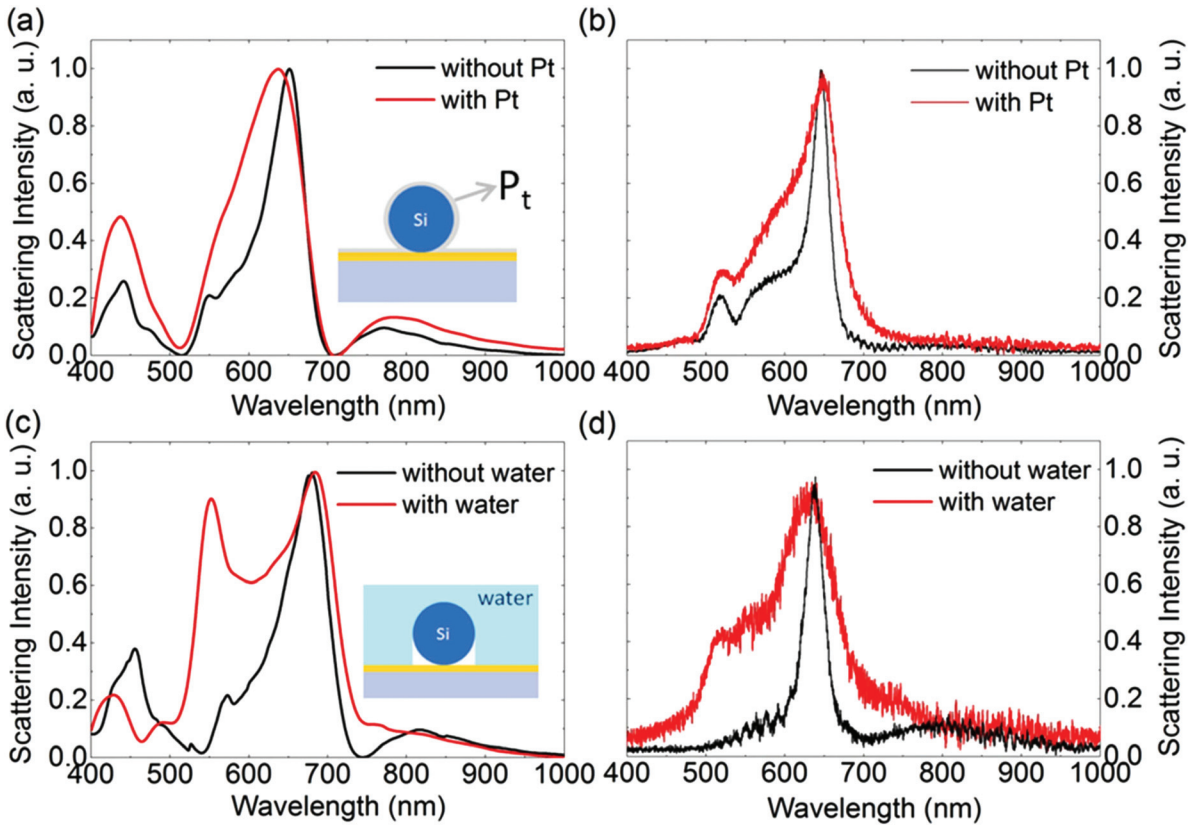

Fig. 6 (a) Simulation results and (b) experimental results for the scattering spectra of a Si NS with D = 202 nm with and without coating of a thin Pt film. The simulation results and experimental results for the scattering spectra of a Si NS with D = 202 nm with and without covering water are shown in (c) and (d), respectively.

case, it has been confirmed that the zero-scattering dip originates from the destructive interference between the new MD and the original one together with its mirror image. This characteristic makes the forward scattering spectrum distinct from the backward one. As a result, the forward scattering spectrum is dominated by the resonant mode with a narrow linewidth which is suitable for sensing applications, as demonstrated in the following. The sharp resonant mode is expected to be sensitive to the surrounding environment of the Si NSs because it is created by the ED of the Si NS and its mirror image. Any change in the surrounding environment will lead to the modification in the resonant mode and the zero-scattering dip (see Fig. S8†). One of the possible applications of the dielectric–metal hybrid system like this is the construction of nanoscale sensors. In order to examine the sensitivity of the resonant mode on the change of the surrounding environment, we performed two experiments. In the first one, an ultrathin (~1 nm) Pt film was coated on the Si NS. In this case, the peak of the resonant mode remains unchanged while a significant broadening of the resonant mode was observed, as shown in Fig. 6(a) and (b). This behavior indicates that the linewidth of the resonant mode is quite sensitive to the refractive index change of the surrounding environment. In the second experiment, the Si NS was covered with water. In this case, a similar behavior was observed if we assumed that water did not enter into the gap between the Si NS and the Au film because of surface tension [see Fig. 6(c) and (d)]. Actually, a slight change in the surrounding environment of the Si NS will result in a significant broadening of the resonant mode and the disappearance of the zero-scattering dip. This feature is quite useful for sensing small specimens attached on the Si NS.

4. Conclusions

In summary, we have investigated numerically and experimentally the interaction of Si NSs with a thin metal film which is clearly reflected in the modification of the forward scattering of Si NSs. A sharp resonant mode and a zero-scattering dip were clearly observed in the modified scattering spectrum. As a result, the forward scattering light modified by the thin metal can exhibit vivid colors with different color indices. It was revealed by numerical simulation that the resonant mode arises from the MD_m while the zero scattering dip originates from the destructive interference between the new MD and original MD together with its mirror image. It was found by numerical simulation that a significant enhancement in both electric and magnetic fields is achieved at the contact point between the Si NS and the metal film. Narrower linewidths can be achieved in Si NEs with their long axes parallel to the metal film. We demonstrated that the change in the surrounding environment results in the significant broadening of the sharp resonant mode and the disappearance of the zero-scattering dip. Our findings indicate the potential applications of dielectric–metal hybrid systems composed of semiconductor NSs and thin metal films in nanoscale plasmonic devices such as displayers, demultiplexers, sensors and lasers.

Acknowledgements

The authors acknowledge the financial support from the National Natural Science Foundation of China (Grant No. 11374109, 11674110, 11674130), the Natural Science Foundation of Guangdong Province, China (Grant No. 2016A030308010, 2016A030306016), and the Science and Technology Planning Project of Guangdong Province, China (Grant No. 2015B090927006).

Notes and references

1 A. I. Kuznetsov, A. E. Miroshnichenko, Y. H. Fu, J. B. Zhang and B. Luk'yanchuk, *Sci. Rep.*, 2012, **2**, 6.
2 A. B. Evlyukhin, S. M. Novikov, U. Zywietz, R. L. Eriksen, C. Reinhardt, S. I. Bozhevolnyi and B. N. Chichkov, *Nano Lett.*, 2012, **12**, 3749–3755.
3 L. Shi, T. U. Tuzer, R. Fenollosa and F. Meseguer, *Adv. Mater.*, 2012, **24**, 5934–5938.
4 J. M. Geffrin, B. García-Cámara, R. Gómez-Medina, P. Albella, L. S. Froufe-Pérez, C. Eyraud, A. Litman, R. Vaillon, F. González and M. Nieto-Vesperinas, *Nat. Commun.*, 2012, **3**, 1171.
5 Y. H. Fu, A. I. Kuznetsov, A. E. Miroshnichenko, Y. F. Yu and B. Luk'yanchuk, *Nat. Commun.*, 2013, **4**, 1527.
6 U. Zywietz, C. Reinhardt, A. B. Evlyukhin, T. Birr and B. N. Chichkov, *Appl. Phys. A: Solid Surf.*, 2013, **114**, 45–50.
7 U. Zywietz, A. B. Evlyukhin, C. Reinhardt and B. N. Chichkov, *Nat. Commun.*, 2014, **5**, 3402.
8 M. Kerker, D. S. Wang and C. L. Giles, *J. Opt. Soc. Am.*, 1983, **73**, 765–767.
9 T. Shibanum, P. Albella and S. A. Maier, *Nanoscale*, 2016, **8**, 14184–14192.
10 J. Y. Tian, Q. Li, Y. Q. Yang and M. Qiu, *Nanoscale*, 2016, **8**, 4047–4053.
11 J. H. Yan, P. Liu, Z. Y. Lin, H. Wang, H. J. Chen, C. X. Wang and G. W. Yang, *ACS Nano*, 2015, **9**, 2968–2980.
12 Y. Tsuchimoto, T. Yano, T. Hayashi and M. Hara, *Opt. Express*, 2016, **24**, 14451.
13 A. E. Miroshnichenko and Y. S. Kivshar, *Nano Lett.*, 2012, **12**, 6459–6463.
14 B. Hopkins, A. N. Poddubny, A. E. Miroshnichenko and Y. S. Kivshar, *Phys. Rev. A*, 2013, **88**, 053819.
15 P. Albella, M. A. Poyli, M. K. Schmidt, S. A. Maier, F. Moreno, J. J. Sáenz and J. Aizpurua, *J. Phys. Chem. C*, 2013, **117**, 13573.
16 H. Wang, P. Liu, Y. L. Ke, Y. K. Su, L. Zhang, N. S. Xu, S. Z. Deng and H. J. Chen, *ACS Nano*, 2015, **9**, 436–448.
17 J. van de Groep and A. Polman, *Opt. Express*, 2013, **21**, 26285–26302.

18 P. Albella, B. Garcia-Cueto, F. Gonzalez, F. Moreno, P. C. Wu, T. Kim, A. Brown, Y. Yang, H. O. Everitt and G. Videen, *Nano Lett.*, 2011, **11**, 3531–3537.
19 E. Xifré-Pérez, L. Shi, U. Tuzer, R. Fenollosa, F. Ramiro-Manzano, R. Quidant and F. Meseguer, *ACS Nano*, 2013, **7**, 664–668.
20 A. E. Miroshnichenko, A. B. Evlyukhin, Y. S. Kivshar and B. N. Chichkov, *ACS Photonics*, 2015, **2**, 1423–1428.
21 Z. Huang, J. Wang, Z. Liu, G. Xu, Y. Fan, H. Zhong, B. Cao, C. Wang and K. Xu, *J. Phys. Chem. C*, 2015, **119**, 28127–28135.
22 I. Sinev, I. Iorsh, A. Bogdanov, D. Permyakov, F. Komissarenko, I. Mukhin, A. Samusev, V. Valuckas, A. I. Kuznetsov, B. S. Luk'yanchuk, A. E. Miroshnichenko and Y. S. Kivshar, *Laser Photonics Rev.*, 2016, **10**, 799–806.
23 G. Lévêque and O. J. F. Martin, *Opt. Express*, 2006, **14**, 9971–9981.
24 J. J. Mock, R. T. Hill, A. Degiron, S. Zauscher, A. Chilkoti and D. R. Smith, *Nano Lett.*, 2008, **8**, 2245–2252.
25 D. Y. Lei, A. I. Fernández-Domínguez, Y. Sonnefraud, K. Appavoo, R. F. Haglund, J. B. Pendry and S. A. Maier, *ACS Nano*, 2012, **6**, 1380–1386.
26 P. Albella, M. A. Poyli, M. K. Schmidt, S. A. Maier, F. Moreno, J. J. Sáenz and J. Aizpurua, *J. Phys. Chem. C*, 2013, **117**, 13573–13584.
27 P. Albella, R. A. de la Osa, F. Moreno and S. A. Maier, *ACS Photonics*, 2014, **1**, 524–529.
28 M. Caldarola, P. Albella, E. Cortés, M. Rahmani, T. Roschuk, G. Grinblat, R. F. Oulton, A. V. Bragas and S. A. Maier, *Nat. Commun.*, 2015, **6**, 7915.
29 R. F. Oulton, V. J. Sorger, T. Zentgraf, R. M. Ma, C. Gladden, L. Dai, G. Bartal and X. Zhang, *Nature*, 2009, **461**, 629–632.
30 P. N. Prasad, *Nanophotonics*, Wiley-Interscience, New York, 2008.
31 S. M. Avdoshenko, C. G. da Rocha and G. Cuniberti, *Nanoscale*, 2012, **4**, 3168–3174.
32 P. E. Sheehan and L. J. Whitman, *Nano Lett.*, 2005, **5**, 803–807.
33 S. Polarz, A. Roy, M. Lehmann, M. Driess, F. E. Kruis, A. Hoffmann and P. Zimmer, *Adv. Funct. Mater.*, 2007, **17**, 1385–1391.
34 X. Duan, Y. Huang, R. Agarwal and C. M. Lieber, *Nature*, 2003, **421**, 241–245.
35 M. Khajavikhan, A. Simic, M. Katz, J. H. Lee, B. Slutsky, A. Mizrahi, V. Lomakin and Y. Fainman, *Nature*, 2012, **482**, 204–207.
36 Y. J. Lu, J. Kim, H. Y. Chen, C. H. Wu, N. Dabidian, C. E. Sanders, C. Y. Wang, M. Y. Lu, B. H. Li, X. G. Qiu, W. H. Chang, L. J. Chen, G. Shvets, C. K. Shih and S. Gwo, *Science*, 2012, **337**, 450–453.
37 S. Strauf and F. Jahnke, *Laser Photonics Rev.*, 2011, **5**, 607–633.
38 J. Y. Suh, C. H. Kim, W. Zhou, M. D. Huntington, D. T. Co, M. R. Wasielewski and T. W. Odom, *Nano Lett.*, 2012, **12**, 5769–5774.
39 Q. Zhang, G. Li, X. Liu, F. Qian, Y. Li, T. C. Sum, C. M. Lieber and Q. Xiong, *Nat. Commun.*, 2014, **5**, 4953.
40 C. Q. Li, C. Y. Zhang, Z. S. Huang, X. F. Li, Q. F. Dai and S. Lan, *J. Phys. Chem. C*, 2013, **117**, 24625–246319.
41 A commercial software developed by Lumerical Solutions Inc. (https://www.lumerical.com) is used for the numerical simulations.
42 S. Noda, A. Chutinan and M. Imada, *Nature*, 2000, **407**, 608–610.
43 I. Rodriguez, L. Shi, X. Lu, B. A. Korgel, R. A. Alvarez-Puebla and F. Meseguer, *Nanoscale*, 2014, **6**, 5666–5670.
44 J. H. Yan, P. Liu, Z. Y. Lin and G. W. Yang, *Nanoscale*, 2016, **8**, 5996–6007.